PROCEEDINGS, Twenty-Fourth Workshop on Geothermal Reservoir Engineering
Stanford University, Stanford, California, January 25-27, 1999
SGP-TR-162

INDUCTIVE SOURCE DESIGN FOR INDUCTIVE FRACTURE DETECTION

E. Cherkaeva[1] and Alan C. Tripp[2]

[1] Department of Mathematics, University of Utah, Salt Lake City, Utah 84112

[2] Department of Geology and Geophysics, University of Utah, Salt Lake City, Utah 84112

ABSTRACT

Traditional inductive logging uses sources whose focussing input waveform does not change with borehole position. While this arrangement facilitates hardware design, the resolution which it provides varies from formation to formation, and is only accidentally optimal for any given sound position. Optimization theory provides a method for designing a distributed inductive borehole source array , which adaptively maximizes the response from an unknown inclusion in a known formation. The adaptive source waveform shaping can be hardwired or can be simulated using simpler source data. The independent information used for the adaptive focussing can be geometric in nature, such as FMS logs, or can be physical property estimates.

Source optimization is particularly important when attempting to detect a subtle feature, such as a fracture in a geothermal field, using triaxial source and triaxial receiver measurements, such as has been suggested in recent literature. A few simple numerical simulations demonstrate why this is so.

INTRODUCTION

Tripp et al. (1999) demonstrate that triaxial source - receiver geometry's and anisotropic formations should be considered for optimal inductive borehole resolution of fracture systems. Unfortunately, the triaxial geometry's and anisotropic formations offer interpretational difficulties which are not encountered in the conventional uniaxial arrays in isotropic materials. The purpose of this paper is to consider some of these problems and to present a possible means of ameliorating their influence.

Moran and Gianzero (1979) offer an extensive investigation of multi-component logging in anisotropic material, which illustrates many of the problems which need to be overcome in a successful system. We will discuss some of their observations briefly.

Although it is necessary to model the response of anisotropic materials in arbitrary geometries, much can be learned about the problems encountered in inductive fracture detection by studying the response of anisotropic whole spaces, contacts between thick anisotropic beds, or a borehole in a anisotropic whole space. Figure 1 illustrates the coordinate system and the source - receiver geometry. For the present section, we assume that the source dipoles are aligned perpendicular and parallel to the bedding.

Moran and Gianzero demonstrate that it is possible to develop a complex apparent conductivity $(\sigma_a)_f = \sigma_r + i(\sigma_x)_f$, where σ_r and $(\sigma_x)_f$ are real quantities. Figure 2 (Moran and Gianzero) illustrates a nomograph for determining σ_h , λ, and hence σ_v from $(\sigma_a)_f$ for thick beds. Figures 3 to 7 illustrate the effects of bed boundaries and boreholes on the bed conductivity values. It is apparent from these figures that bed boundaries and boreholes can have a significant impact on the accuracy of the formation conductivity estimate.

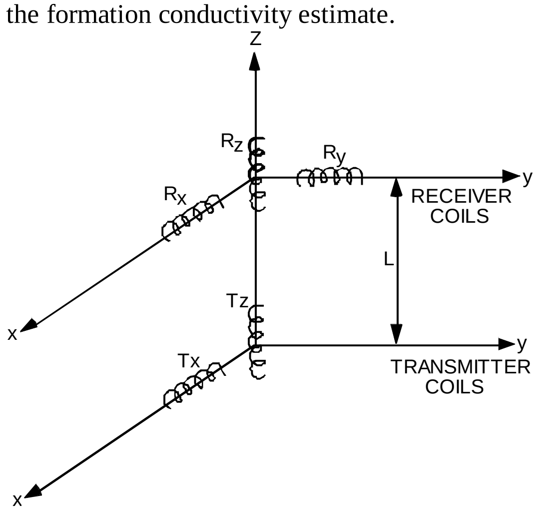

Figure 1

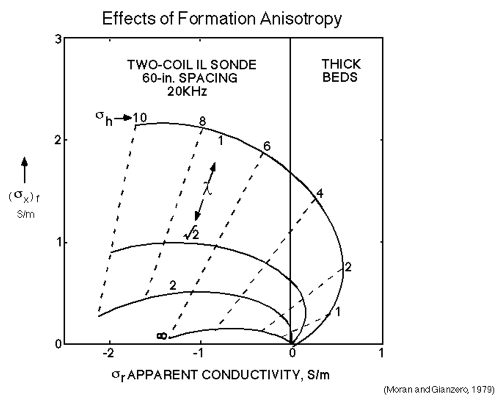

Figure 2

Previous literature on triaxial inductive logging of anisotropic material have tied the effectiveness of the technique to overcoming the biasing effects of the borehole and other inhomogeneities (Moran and Gianzero,1979; Nekut, 1994; Howard, 1981). One possible means of overcoming this problem is to use focussing arrays to lessen the effect of the borehole and other known effects. Cherkaeva and Tripp, 1996a,b) discuss an adaptive focussing technique which may be useful in overcoming the effects of the borehole or other inhomogeneities detectible using independent information.

FOCUSSED ARRAYS IN INDUCTION LOGGING

The goal of induction logging is to measure the fields H in a borehole which are induced by a set of sources J_m and subsequently deduce the spatially varying function σ. We will maximize the resolution of σ vis-à-vis a particular a-priori model by optimizing the magnitudes of the impressed currents.

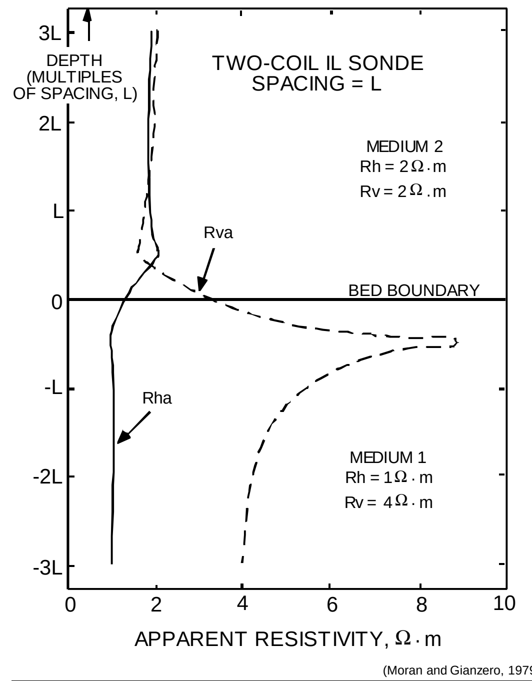

Figure 3

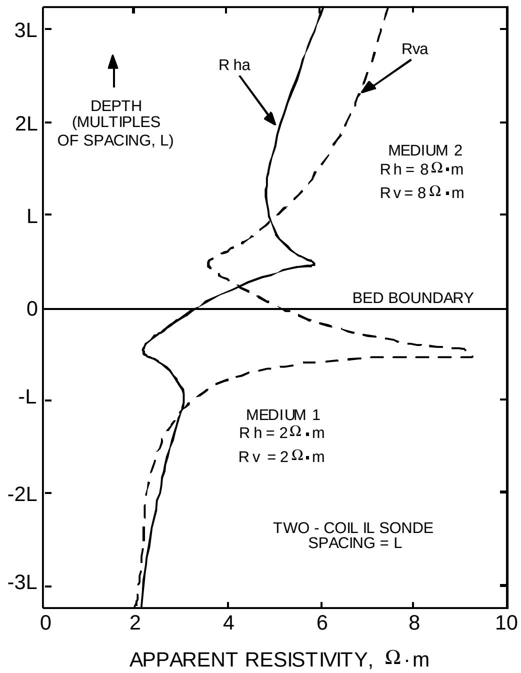

(Moran and Gianzero, 1979)

Figure 4

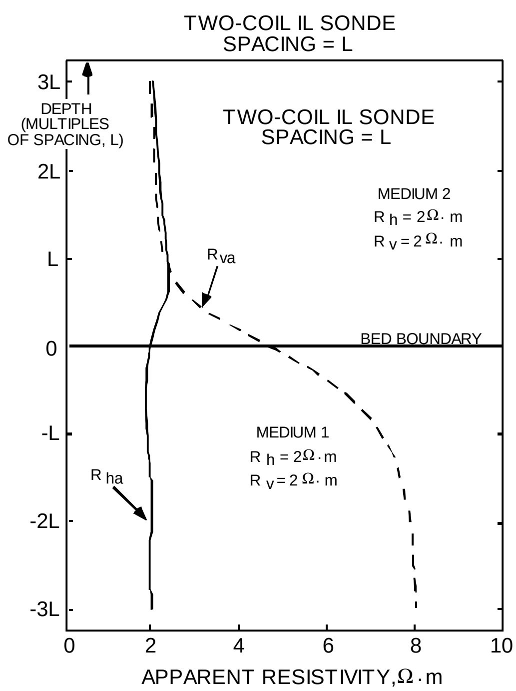

(Moran and Gianzero, 1979)

Figure 5

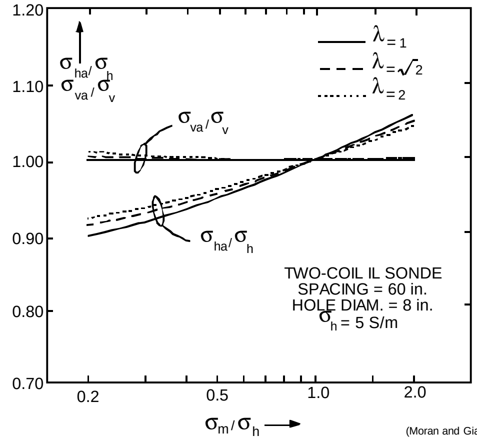

(Moran and Gianzero, 1979)

Figure 6

In the following, we assume that the source and receiver are co-axial. Similar derivations could be made for other orientations.

Suppose that the background medium is characterized by the conductivity distribution σ_0 , with the fields E^0 and H^0, generated by the same magnetic currents J_m, while the received fields are $H^0{}_z$. The difference between the measured and the background fields is due to the difference in conductivity distributions corresponding to the real and the background media. The optimal impressed magnetic source array is that array which maximizes the difference between the measured field due to the real medium and the field calculated from the a-priori model.

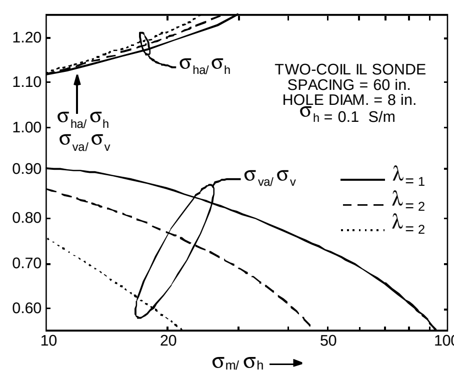

(Moran and Gianzero, 1979)

Figure 7

Hence, suppose that an array of axially directed magnetic dipoles is arranged along a borehole axis. Assume that the n dipoles are indexed by i and that $\mathbf{J} = [\, J_1, J_2, ..., J_n]^T$ is a vector of magnetic moments. The measured fields for the perturbed conductivity σ and the background conductivity σ_0 are related to an arbitrary magnetic dipole moment $\mathbf{j}$ by the linear operators $\mathbf{L}\sigma$ and $\mathbf{L}\sigma_0$. If we assume that the number of transmitters is equal to the number of receivers, and that an array of magnetic dipoles of varying magnitude can be represented as $\mathbf{f} = \Sigma\, \alpha_k \mathbf{j}^k$, where $\mathbf{j}^k{}_i = \delta_{ik}$, then we wish to maximize the quantity

$$\lambda = \| (\mathbf{L}\sigma - \mathbf{L}\sigma_0)\, \Sigma\, \alpha_k \mathbf{j}^k \|,$$

where the norm is the Euclidean sum of squares, subject to the constraint that $\Sigma\, \alpha_k = 1$. The λ and the α_k which solve this optimization problem give the solution to the eigenvalue problem

$$\lambda^{\sim}\, \mathbf{a} = (\mathbf{L}\sigma - \mathbf{L}\sigma_0)\, \mathbf{a},$$

where $\mathbf{a} = \Sigma\, \alpha_k \mathbf{j}^k$ and $|\lambda^{\sim}| = \lambda$.

In this formulation, the dipole array magnitude is normalized since an increase in transmitter power leads to an increase in anomaly magnitude irregardless of array relative weighting.

This eigenvalue formulation can be solved numerically using SVD from LINPACK to give a series of ranked solutions

$$\{ \lambda_1, \mathbf{a}^1\}, \{ \lambda_2, \mathbf{a}^2\}, ..., \{ \lambda_n, \mathbf{a}^n\},$$

where $\mathbf{a}^i = \{\alpha_k{}^i\}$.

The magnetic current array $\mathbf{J}_1 = \Sigma\, \alpha_k{}^i\, \mathbf{j}^k$ corresponding to the maximal eigenvalue λ_1 gives the most information about the conductivity perturbation of any current array. The remaining eigenvalues form a monotonically decreasing sequence, corresponding to arrays which give lesser amounts of information concerning the conductivity distribution. Including them in a conductivity inversion will contribute additional information as long as the associated eigenvalues are above the data noise, at the expense of additional data collection time.

The efficacy of the method can be illustrated using a computer simulation. For this simulation, the EM forward response was computed using the algorithm SYSEM (Xiong and Tripp, 1993, 1995a,b).

Figure 8 illustrates the model which is considered. This model consists of a 1 m fracture zone of horizontal resistivity 100 Ω - m, embedded in a background unit of horizontal resistivity 10 Ω - m. Note that this is a much m ore difficult target than the regular "conductive fracture" zone model, and could correspond to a case in which a particular lithologic zone has fractures which parallel the borehole. To make the problem even more difficult, we assume that there is an invasion zone of horizontal resistivity 1 Ω - m. Again , a ll of the units have arbitrary vertical resistivity - the vertical transmitter array shown in the figure has no sensitivity to vertical resistivity components.

In each model, the borehole and bounding media attributes are known, as well as the resistivity and thickness of the invasion zone. The 100 Ω - m zone behind the invasion zone is the target zone and all array optimizations are designed to optimize this unknown region given the knowledge about the rest of the model. The transmitting and receiving dipoles were spaced at 1m intervals, with a total of 15 of each. The locations of some of the transmitting dipoles are shown by the arrows. The receiver locations coincide with the transmitter locations. We assume that all transmitters will fire in-phase with each other and that each receiver will record the response due to each of the transmitters. Alternately, we could represent the measured response as a weighted sum of the responses due to each separate transmitter. In either case, our task is to find the relative transmitter weighting which maximizes the response of the 100 Ω - m zone, assuming an a-priori model where all the other model parameters are known and the 100 Ω - m zone is thought to be 10 Ω - m.

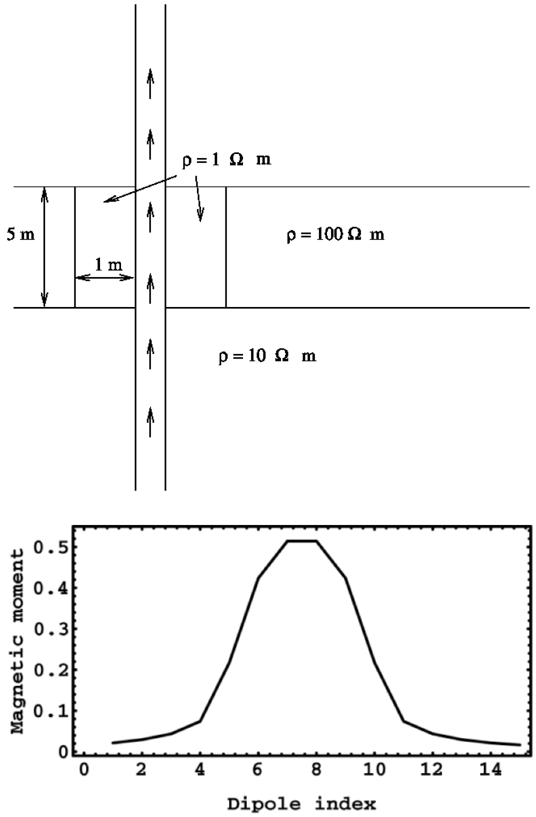

Figure 8: A cross-section of the model (top) and the optimal distribution of the moments of magnetic dipoles (bottom).

Figure 8 shows the optimal transmitter weighting for Model 1. Obviously, the array weighting is using the invasion zone to "focus" energy into the resistive zone. Figure 9 illustrates the difference in response due to the focussing array and an array in which all dipoles are equally weighted.

Figures 10 through 13 illustrate contours of the H_Z and the E_y responses for the optimized transmitter array and uniformly weighted arrays for an x-y cross-section containing the borehole axis. In all plots it is apparent that the focussing array leads to an improved field concentration in the fracture zone.

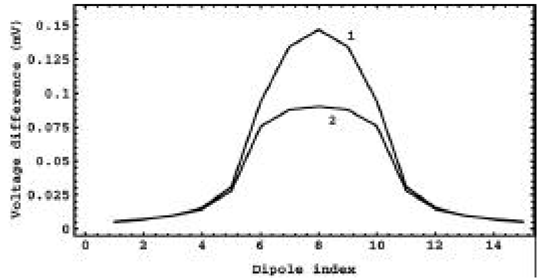

Figure 9

Another way of focussing energy is to modify adaptively the source waveform. Cherkaeva and Tripp (1996c) discuss such an application for a surface-to-borehole survey for a buried anisotropic layer.

DISCUSSION AND CONCLUSIONS

We have demonstrated that adaptive array focussing can optimize resolution of an unknown feature in the presence of known, masking features. This theory should be generalizable to a triaxial measurement, where the borehole itself represents the "masking unit". Although in this work, the array weights are developed supposing that all transmitters of the array are in-phase, phased array weights are possible and would be better in maximizing resolution of the conductivity of the formation.

ACKNOWLEDGEMENTS

Financial support for this study was provided by the U.S. Department of Energy under grant DE-FG03-93ER14313. Such support does not constitute an endorsement of the views expressed in this publication.

REFERENCES

Cherkaeva, E. and Tripp, A.C., 1998, Optimal focussing in inductive logging: Submitted for Presentation at the 68th Annual SEG Meeting.

deCarvalho, P.R. and Verma, O.P., 1994, Coplanar coil system in electromagnetic induction well-logging tool: SPWLA 35th Annual Logging Symposium.

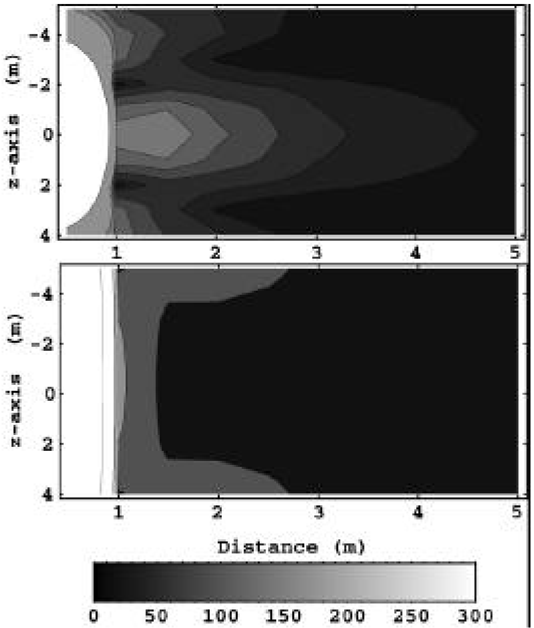

Figure 10: Cross-plots of the amplitude of *Hz* for the optimal weighting (top) and uniform weighting (bottom). The frequency of excitation is 1kHz. The contours are in units of .1 milliAmps/m.

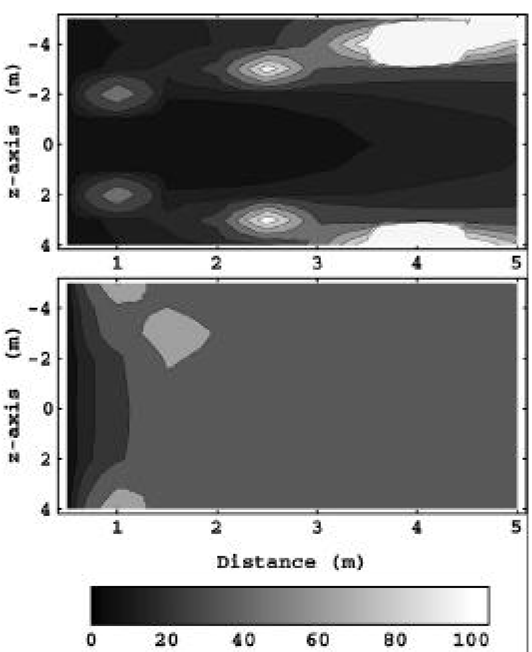

Figure 11: Cross-plots of the phase of *Hz* for the optimal weighting (top) and uniform weighting (bottom). The frequency of excitation is 1 kHz. The contours are in mrad.

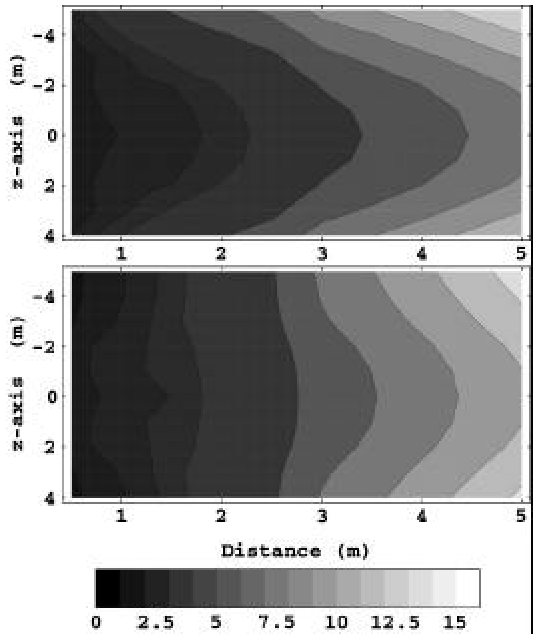

Figure 12: Cross-plots of the amplitude of *E*y for the optimal weighting (top) and uniform weighting (bottom). The frequency of excitation is 1 kHz. The contours are in units of .01mV/m.

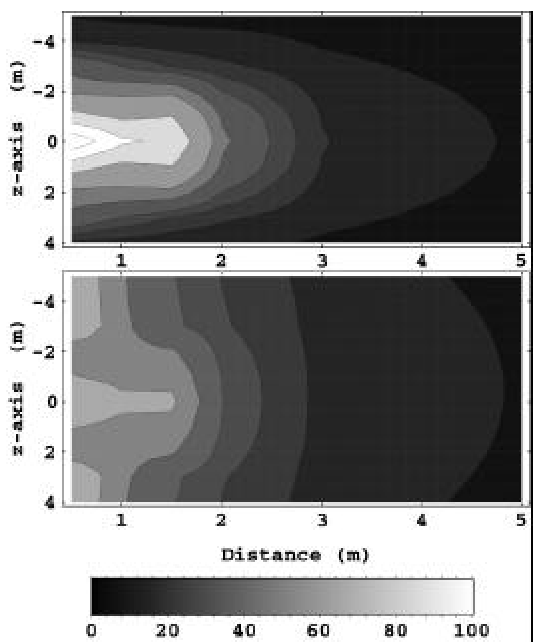

Figure 13. Cross-plots of the phase of *Ey* for the optimal weighting (top) and uniform weighting (bottom). The frequency of excitation is 1 kHz. The contours are in mrad.

Howard, A.Q., Jr., 1981, Induction logging for vertical structures in the presence of a borehole fluid: Geophysics, v. 46, 68-75.

Moran, J.H. and Gianzero, S., 1979, Effects of formation anisotropy on resistivity logging measurements: Geophysics, v. 44, 1266-1286.

Nekut, A.G., 1994, Anisotropy induction logging: Geophysics, v. 59, 345-350.

Sato, T., Osato,K., Takasugi, S., and Uchida, T., 1996, Development of the Multi-Frequency Array Induction Logging (MAIL) tool: Geothermal Resources Council Transactions, v. 20, 637-642.

Tripp, A.C., Bruhn, R., Jarrard, R.D., and Brown, S., 1999, Inductive detection of fractures in geothermal systems - Petrophysical aspects and geophysical implications: Proceedings of the Twenty -fourth Workshop on Geothermal Reservoir Engineering.

Wilt, M., Takasugi, S., Uchida, T., Kasameyer, P., Lee, K., and Lippmann, M., 1997, Fracture mapping in geothermal fields with long-offset induction logging: Proceedings of the Twenty-Second Workshop on Geothermal Reservoir Engineering, Stanford University.

Wilt, 1998, Pers. Comm.

Xiong, Z. and Tripp, A.C., 1993, Scattering matrix evaluation using spatial symmetry in electromagnetic modeling, Geophysics Journal International, v. 114, 459-464.

Xiong, Z. and Tripp, A.C., 1995a, A block iterative algorithm for 3-D electromagnetic modeling using integral equations with symmetrized substructures: Geophysics, v. 60, no. 1, 291-295.

Xiong, Z. and Tripp, A.C., 1995b, Electromagnetic modeling of large structures in layered earth's using integral equations: Radio Science, v. 30, no. 4, 921-929.